Topological projected transport of colloids in quasicrystals

Bachelor thesis

submitted by

Timo Lebeda

Bayreuth, 28.11.2016

Supervisors: Dr. Daniel de las Heras, Prof. Thomas Fischer and Prof. Matthias Schmitt

Contents

1 Introduction

This thesis are the physical part of an interdisciplinary project in maths and physics, containing two Bachelor thesis, this one and [2], both submitted by myself.
In the mathematical part we discuss the properties of quasicrystals and how they can be constructed, while in the physical part we study the transport of colloids in quasicrystals.
Both parts are explicit connected by the construction of the quasicrystal that we use for the simulations, what is also an example for the construction of a Penrose tiling. This construction is part of this thesis.
Moreover there is an implicit connection of both parts, since we will use mathematical properties of the constructed quasicrystal to learn something about the transport of colloids, for example the so-called inner space. The inner space is a tool which is generated in the mathematical construction of cut-and-project quasicrystals, but there is no physical interpretation for it. Thus it is necessary to understand the used construction method mathematically, if we want to understand the transport of colloids in such materials.
Due to the close connection of both thesis, they are both studied in one project and we will often refer to the mathematical thesis.

In particular, we construct a Penrose tiling of the plane using both, the multigrid method and the cut-and-project mehtod. This construction is based on the results we derived in the sections 4.3 and 4.4 of the mathematical part, see [2], and is thus a more detailed example for the construction of two-dimensional cut-and-project quasicrystals.
Moreover we use the mathematical properties of the constructed quasicrystal to study the transport of colloids in quasicrystals.

Our motivation in the physical part is to transfer the results, M.Loehr et al. found for the topological protected transport of colloids in crystals by external magnetic fields, cf. [3] and [1], to the transport of colloids in quasicrystals. The transport in crystals leads to the problem that one can only move all particles into the same direction, since all (unit-)cells are equivalent.
In opposite to that in quasicrystals every cell (tile) is different, because no two cells can have exactly the same environment due to the lack of translational symmetry. Thus we hope to be able to transport two particles independent of each other into predicted directions along the quasicrystal.
Since a generalization of the hole results of Loehr et al. would be far too much for this Bachelor thesis, we restrict ourselves to show, how one single colloid can be transported along the quasicrystal, and give two ideas, how one could controll the simultanious transport of two or more colloids.
Therefor we simulate the movement of diamagnetic colloids in the constructed Penrose quasicrystal, driven by an external magnetic field, using Brownian dynamics.

In particular, we construct the Penrose tiling in section 2.
The simulation setup and some notation will be introduced in section 3.
We calculate the external field that transports a single colloid along a given path through the quasicrystal in section 4.
In section 5 we discuss two possibilities how two or more particles could be transported independent along the quasicrystal. First we use the results we derived for the transport of a single particle and give a theoretical method, which we think is not useful in practice, since it needs a huge amount of calculation. The second idea is to use the fact that points (i.e. vertices of the Delone tiling), whose projections onto the inner space $\mathcal{E}^\perp$ are close to each other, have a similar environment in the quasicrystal and thus the external fields, which move colloids inside the corresponding tile of the Voronoi tiling into a given direction, should be similar.

2 Construction of the quasicrystal used in the simulations

Following the multigrid method that we introduced in [2], section 4.4, we will construct the quasicrystal or, to more exact, the quasicrystallographic tiling that we use in the simulations. In particular we will construct a Pentagrid and dualize it to obtain a Delone tiling and the corresponding Voronoi tesselation of the plane. Moreover we will use the cut-and-project method to construct the inner space $\mathcal{E}^{\perp}$. We will see that the tiling we construct is a Penrose tiling of the plane.

Since we construct a tiling of the plane, we have $n = 2$.
As first step we define the five grid vectors $\vec{\epsilon}_0, \ldots, \vec{\epsilon}_4$ by

$$\vec{\epsilon}_j := \left(\cos\left(\frac{2\pi j}{5}\right), \sin\left(\frac{2\pi j}{5}\right)\right), j = 0, 1, 2, 3, 4.$$

For the shift vector we choose

$$\vec{\gamma} = (0, \varepsilon, 2\varepsilon, 3\varepsilon, -6\varepsilon)$$

with $\varepsilon = 0,0001$.

One can show that

Theorem 2.1: If the shift vector $\vec{\gamma}$ is regular and $\sum_{j=0}^{4} \vec{\gamma}_j \in \mathbb{Z}$, the dual tiling (to the Pentagrid) is a Penrose tiling.
Proof: See [4] Theorem 6.4.
Note that in [4] the grids are labeled by $\mathbb{Z} + \frac{1}{2}$ instead of $\mathbb{Z}$ and thus the condition there is that the sum must be $\frac{1}{2} \mod 1$.

Corollary 2.2: The quasicrystal that we use in the simulations is a Penrose tiling of the plane.
Proof: $\vec{\gamma}$ is regular and

$$\sum_{j=0}^{4} \vec{\gamma}_j = 0.$$

□

In [2], section 4.4, we derived the mesh condition:

$$l_j - 1 < \langle \vec{x}, \vec{\epsilon_j} \rangle_2 + \gamma_j < l_j, \ \forall j \in \{0, \ldots, k-1\}.$$

It implicates that $\lceil \langle \vec{x}, \vec{\epsilon_j} \rangle_2 + \gamma_j \rceil = const. =: k_j$ for every point $\vec{x}$ inside a given mesh. Thus the mesh is uniquely labeled by the 5-tuple $(k_0, \ldots, k_4)$. The corresponding vertex of the dual tiling has the coordinates

$$\sum_{j=0}^{4} k_j \vec{\epsilon}_j.$$

In [2], section 4.4, we found that at most two grids can meet at any point, and that each intersection in the Pentagrid corresponds to a tile in the dual tiling and vice versa. Let T be the tile corresponding to the intersection of two lines k_r and k_s in grids r and s, respectively, where $0 \leq r < s \leq 4$.

As basis of our coordinate system we choose the two vectors

$$\vec{x}_r = \frac{\left(\sin\left(\frac{2\pi s}{5}\right), -\cos\left(\frac{2\pi s}{5}\right)\right)}{\left\langle\left(\sin\left(\frac{2\pi s}{5}\right), -\cos\left(\frac{2\pi s}{5}\right)\right), \left(\cos\left(\frac{2\pi r}{5}\right), \sin\left(\frac{2\pi r}{5}\right)\right)\right\rangle_2}$$

and

$$\vec{x}_s = \frac{\left(-\sin\left(\frac{2\pi r}{5}\right), \cos\left(\frac{2\pi r}{5}\right)\right)}{\left\langle\left(-\sin\left(\frac{2\pi r}{5}\right), \cos\left(\frac{2\pi r}{5}\right)\right), \left(\cos\left(\frac{2\pi s}{5}\right), \sin\left(\frac{2\pi s}{5}\right)\right)\right\rangle_2},$$

which are the lattice vectors reciprocal to $\vec{\epsilon}_r$ and $\vec{\epsilon}_s$, respectively.
Then our points are

$$\vec{x} = (kr - \gamma_r)\vec{x}_r + (ks - \gamma_s)\vec{x}_s$$

with $kr, ks \in \mathbb{Z}$. In order to keep the calculation time small, we set

$$-6 \leq kr, ks \leq 6.$$

If one needs a greater patch of the tiling, one can allow more values of kr and ks.

Now we can calculate k_j for $0 \leq j \leq 4$ and a given point $\vec{x}$:

$$k_j := \lceil \langle \vec{x}, \vec{\epsilon_j} \rangle_2 + \gamma_j \rceil \in \mathbb{Z}.$$

Note that $k_r = kr$ and $k_s = ks$.
We can say that $T = (r, s, \vec{k})$, $\vec{k} = (k_0, \ldots, k_4)$.
One vertex of the tile T is

$$T_1 = \sum_{j=0}^{4} k_j \vec{\epsilon}_j.$$

Since T belongs to the orthogonally dual tiling of the Pentagrid, its edges point into the directions of the star vectors $\vec{\epsilon}_r$ and $\vec{\epsilon}_s$. In particular the other three vertices are

$$\begin{aligned} T_2 &= T_1 + \vec{\epsilon}_r, \\ T_3 &= T_2 + \vec{\epsilon}_s, \\ T_4 &= T_3 - \vec{\epsilon}_r. \end{aligned}$$

Equivalent, we can say that the four vertices $T_1, \ldots, T_4$ of the tile T correspond to the four 5-tuples $\vec{k}^1 = (k_0, \ldots, k_4)$, $\vec{k}^2 = \vec{k}^1 + \vec{e}_r$, $\vec{k}^3 = \vec{k}^1 + \vec{e}_r + \vec{e}_s$ and $\vec{k}^4 = \vec{k}^1 + \vec{e}_s$. Saying $\vec{k}^i = (k_0^i, \ldots, k_4^i)$, we have

$$T_i = \sum_{j=0}^{4} k_j^i \vec{\epsilon}_j, \;\; i = 1, 2, 3, 4.$$

In order to draw the tiling, we connect the four vertices of each tile T and plot them.
The resulting **Delone tiling** is the purple tiling in figure 1.

The construction of the Voronoi tesselation is standard: We construct the Voronoi cells for all vertices of the Delone tiling and plot them all together. The resulting **Voronoi tiling** is the green one in figure 1.

Indeed we have only constructed finite patches of both tilings, but this is enough for the simulations, since our particles won't move too far.

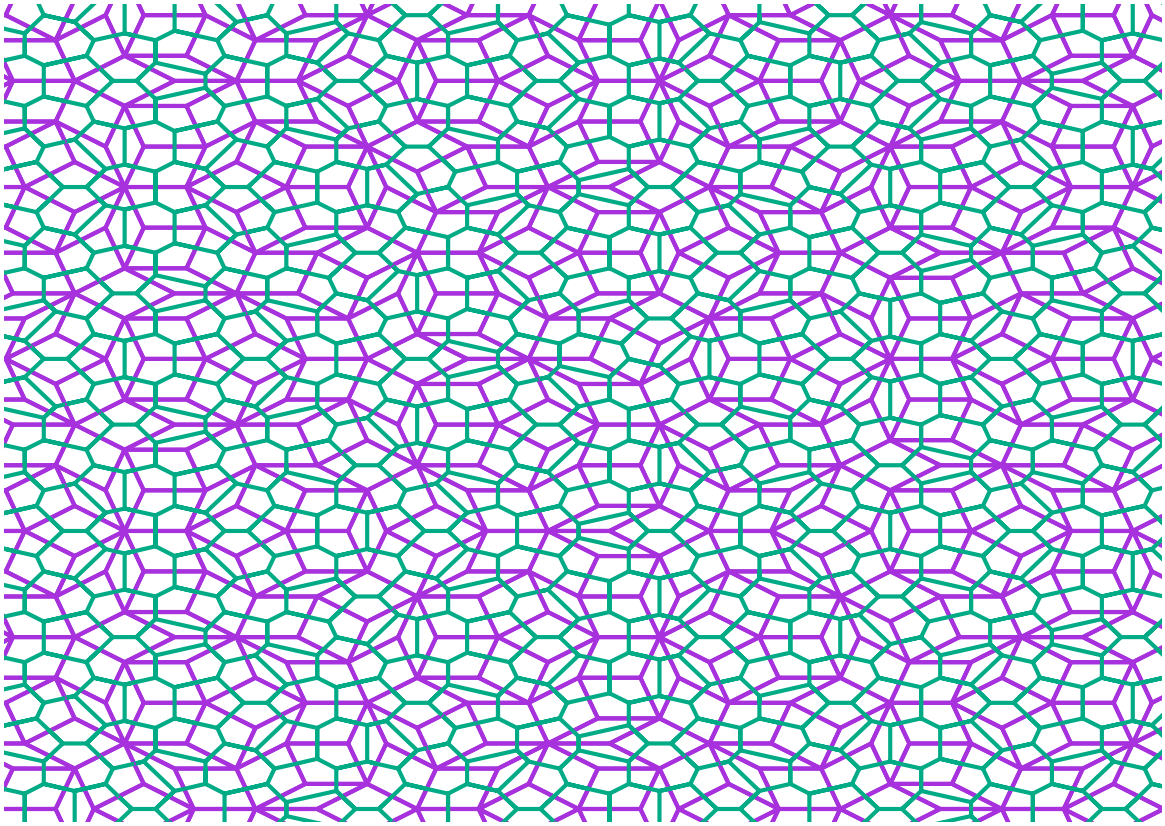

Figure 1: The constructed Delone tiling (purple) and the corresponding Voronoi tiling (green).

In order to construct the inner space $\mathcal{E}^\perp$, we interpret the 5-tuples $(k_0, \ldots, k_4)$ as points of the 5-dimensional standard lattice $\mathcal{I}_5$ and the Delone tiling as the (canonical) projection of these points, in the way we discussed in [2], section 4.4.
What we need therefor is the map $\Pi^\perp : \mathcal{I}_5^p \to \mathcal{E}^\perp, (k_0, \ldots, k_4) \mapsto \Pi^\perp((k_0, \ldots, k_4))$, i.e. the projection onto inner space. Following [4] Chapter 2.6.3, we will derive this map, which is obviously a matrix in $\mathbb{R}^{5\times 3}$. Note that we ignore the difference between row and column vectors at this point.

Since we use canonical projection, the window is the Voronoi cell of $\mathcal{I}_5$, a 5-dimensional hypercube $\mathcal{Q}_5$, compare [2], section 4.4. The 'body diagonal' of $\mathcal{Q}_5$ is the line segment from $(0, 0, 0, 0, 0)$ to $(1, 1, 1, 1, 1)$, the corresponding vector is $\vec{w} = (1, 1, 1, 1, 1)$. 5-fold rotation ϕ about $\vec{w}$ is a symmetry of the hypercube, since it permutes the five basis vectors $\vec{e}_j$, $j = 1, \ldots, 5$ cyclically. With respect to this basis, the rotation matrix is

$$\mathcal{A} = \begin{pmatrix} 0 & 0 & 0 & 0 & 1 \\ 1 & 0 & 0 & 0 & 0 \\ 0 & 1 & 0 & 0 & 0 \\ 0 & 0 & 1 & 0 & 0 \\ 0 & 0 & 0 & 1 & 0 \end{pmatrix}.$$

The eigenvalues of $\mathcal{A}$ are the fifth roots of unity,

$$1, \xi, \xi^2, \xi^3, \xi^4,$$

where

$$\xi^j = \exp\left(\frac{2\pi i j}{5}\right),\ j = 0, \ldots, 4.$$

The only real eigenvalue is 1, the others are complex. In particular ξ is the complex conjugate of ξ^4 and ξ^2 is the complex conjugate of ξ^3. This implicates that $\mathbb{R}^5$ decomposes into two 2-dimensional planes $\mathcal{E}$ and $\mathcal{E}'$, both stable under ϕ, both totally irrational, and both orthogonal to the fixed space Δ generated by $\vec{w}$ (and to one another).
We have $\mathcal{E}^\perp = \mathcal{E}' \oplus \Delta$. Note that $\mathcal{E}^\perp$ is not totally irrational, since Δ contains the multiples of $\vec{w}$. Indeed $\Pi^\perp(\mathcal{I}_5^p)$ does not fill $\mathcal{E}^\perp$ densely, but it consists of translates of densely filled planes, compare figure 2.

Obviously, $\vec{w}$ is an eigenvector belonging to the eigenvalue 1. The eigenvectors belonging to ξ^j, $j = 1, \ldots, 4$ are multiples of

$$\vec{v}_j = (1, \xi^j, \xi^{2j}, \xi^{3j}, \xi^{4j}).$$

Note that

$$\langle \vec{w}, \vec{v}_j \rangle_2 = 0,\ j = 1, \ldots, 4$$

and

$$\langle \vec{v}_i, \vec{v}_j \rangle_2 = 0,\ i \neq j.$$

Thus $\vec{v}_1$ and $\vec{v}_4$ span a plane orthogonal to the plane spanned by $\vec{v}_2$ and $\vec{v}_3$, and both planes are orthogonal to $\vec{w}$.
The $\vec{v}_1$, $\vec{v}_4$ plane contains the real eigenvectors

$$\vec{v}_1 + \vec{v}_4 = 2\left(1, \cos\left(\frac{2\pi}{5}\right), \cos\left(\frac{4\pi}{5}\right), \cos\left(\frac{4\pi}{5}\right), \cos\left(\frac{2\pi}{5}\right)\right)$$

and

$$i(\vec{v}_1 - \vec{v}_4) = 2\left(0, \sin\left(\frac{2\pi}{5}\right), \sin\left(\frac{4\pi}{5}\right), -\sin\left(\frac{4\pi}{5}\right), -\sin\left(\frac{2\pi}{5}\right)\right),$$

while the $\vec{v}_2$, $\vec{v}_3$ plane contains the real eigenvectors

$$\vec{v}_2 + \vec{v}_3 = 2\left(1, \cos\left(\frac{4\pi}{5}\right), \cos\left(\frac{2\pi}{5}\right), \cos\left(\frac{2\pi}{5}\right), \cos\left(\frac{4\pi}{5}\right)\right)$$

and

$$i(\vec{v}_2 - \vec{v}_3) = 2\left(0, -\sin\left(\frac{4\pi}{5}\right), \sin\left(\frac{2\pi}{5}\right), -\sin\left(\frac{2\pi}{5}\right), \sin\left(\frac{4\pi}{5}\right)\right).$$

Let $\vec{u}_1, \vec{u}_2, \vec{u}_3, \vec{u}_4$ be the unit vectors parallel to $\vec{v}_1 + \vec{v}_4$, $\vec{v}_2 + \vec{v}_3$, $i(\vec{v}_2 - \vec{v}_3)$ and $i(\vec{v}_1 - \vec{v}_4)$ (in particular this means to scale all four vectors by $\frac{1}{2}\sqrt{\frac{2}{5}}$), and let $\vec{u}_5 = \frac{1}{\sqrt{5}}\vec{w}$. Then $\vec{u}_1, \ldots, \vec{u}_5$ is an orthonormal basis of eigenvectors of the rotation ϕ.

The matrices of the projectors onto $\mathcal{E}$ (the $\vec{v}_1$, $\vec{v}_4$ plane) and $\mathcal{E}^\perp$ (the direct sum of the $\vec{v}_2$, $\vec{v}_3$ plane and $\vec{w}$), Π and $\Pi^\perp$, are thus

$$\Pi \sim \begin{pmatrix} \vec{u}_1 \\ \vec{u}_4 \end{pmatrix}$$

and

$$\Pi^\perp \sim \begin{pmatrix} \vec{u}_2 \\ \vec{u}_3 \\ \sqrt{5}\vec{u}_5 \end{pmatrix}.$$

Now we have an explixit expression for $\Pi^\perp$ and can easily construct the inner space $\mathcal{E}^\perp$ as

$$\mathcal{E}^\perp = \Pi^\perp(\mathcal{I}_5^p).$$

We use $\sqrt{5}\vec{u}_5$ instead of the canonical $\vec{u}_5$, because this ensures that the z-components of the points in $\mathcal{E}^\perp$ are integers. This doesn't change the symmetry of $\mathcal{E}^\perp$, because $\mathcal{E}^\perp$ consists of four planes parallel to the x-y-plane.
The inner space we have calculated is shown in figure 2.
Note that we have found a projection onto $\mathcal{E}$ by the way, which enables us to project the vertices of the Delone tiling, which are exactly the images of $\mathcal{I}_5^p$ under Π, onto the inner space $\mathcal{E}^\perp$ by applying $\Pi^\perp \circ \Pi^{-1}$.

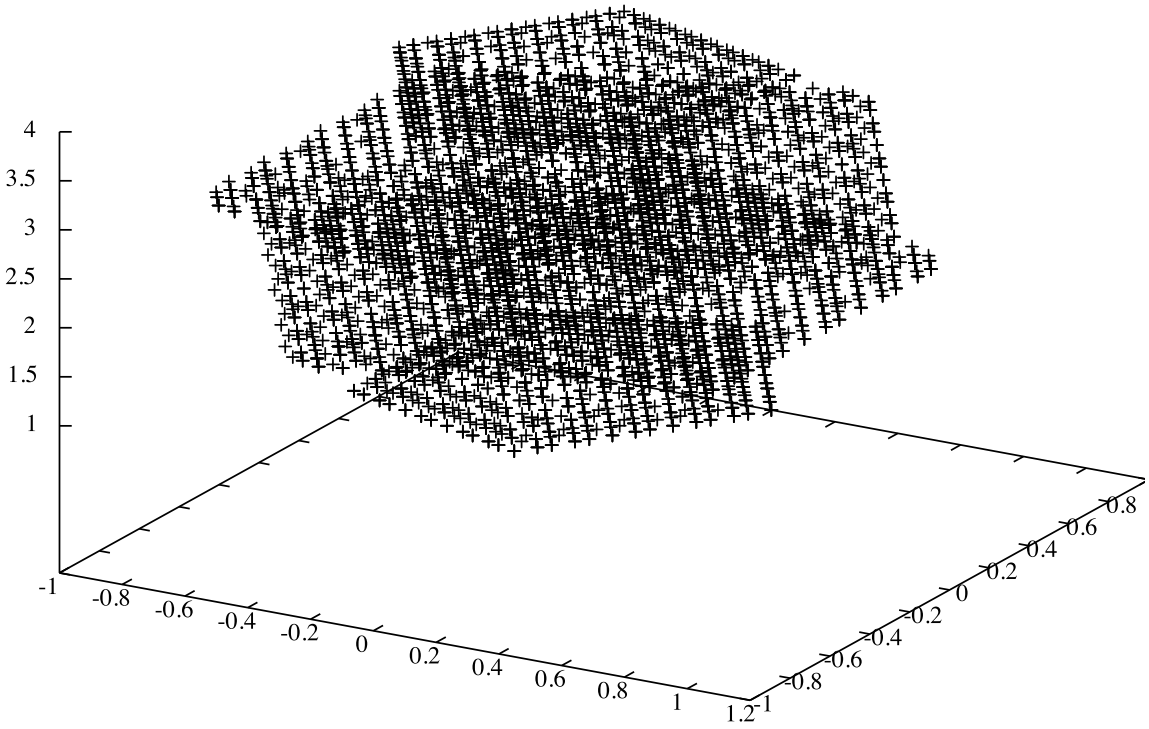

Figure 2: The constructed inner space $\mathcal{E}^\perp$.

As earlier stated, the inner space consists of translates of densely filled planes. In particular there are four planes with z-coordinates $1, 2, 3, 4$. We say that the value of the z-coordinate of a plane is its level.
Why do exactly these four levels appear? The reason is the mesh condition (2).
Let $\vec{k} = (k_0, \ldots, k_4) \in \mathcal{I}_5^p$. If we add the five inequalities in (2), we have

$$\sum_{j=0}^{4} k_j - 5 < \sum_{j=0}^{4} \langle \vec{x}, \vec{\epsilon_j} \rangle_2 + \sum_{j=0}^{4} \gamma_j < \sum_{j=0}^{4} k_j.$$

Since $\sum_{j=0}^{4} \gamma_j = 0$ and $\sum_{j=0}^{4} \vec{\epsilon_j} = 0$, we obtain

$$\sum_{j=0}^{4} k_j - 5 < 0 < \sum_{0=1}^{4} k_j$$

and thus

$$\sum_{j=0}^{4} k_j \in \{1, 2, 3, 4\}.$$

The z-component of $\Pi^{\perp}(\vec{k})$ is

$$\left(\Pi^{\perp}(\vec{k})\right)_z = \langle \sqrt{5}\vec{u}_5, \vec{k} \rangle_2 = \langle \vec{w}, \vec{k} \rangle_2 = \sum_{j=0}^{4} k_j,$$

and consequently

$$\left(\Pi^{\perp}(\vec{k})\right)_z \in \{1, 2, 3, 4\}.$$

Note that two adjacient vertices of the Delone tiling are never projected onto the same level. Moreover one can show that the vertices of a given tile T are either projected onto the levels $(1, 2, 3, 2)$ or $(2, 3, 4, 3)$:
Let, as before, $T_1, \ldots, T_4$ be the vertices of the tile T and $\vec{k}^i = (k_0^i, \ldots, k_4^i)$, $i = 1, 2, 3, 4$ the corresponding 5-tuples. If we set

$$a := \sum_{j=0}^{4} k_j^1,$$

we obtain

$$\sum_{j=0}^{4} k_j^2 = \sum_{j=0,\ j\neq r}^{4} k_j^1 + (k_r^1 + 1) = a + 1,$$

$$\sum_{j=0}^{4} k_j^3 = \sum_{j=0,\ j\neq s}^{4} k_j^2 + (k_s^2 + 1) = a + 2,$$

$$\sum_{j=0}^{4} k_j^4 = \sum_{j=0,\ j\neq r}^{3} k_j^3 + (k_r^3 - 1) = a + 1.$$

Since $a, a + 2 \in \{1, 2, 3, 4\}$, the possible values of a are $a = 1$ and $a = 2$, i.e. the combinations $(1, 2, 3, 2)$ and $(2, 3, 4, 3)$, respectively.

In the following section we will use the constructed quasicrystal to study the transport of colloids in quasicrystals.

3 Simulation setup

We call the two-dimensional space $\mathcal{A}$ in which the colloids move action space and denote the coorindates by $\vec{x}_{\mathcal{A}}$. The five reciprocal lattice vectors are equal to the five star vectors, upto a scaling factor:

$$\vec{q_j} = q\vec{\epsilon_j} = q\left(\cos\left(\frac{2\pi j}{5}\right), \sin\left(\frac{2\pi j}{5}\right)\right), j = 1, 2, 3, 4, 5.$$

We use an external magnetic field $\vec{H}_{ext}$ with fixed absolute value. Thus we can describe the field in spherical coordinates with two angles:

$$\vec{H}_{ext}(\theta, \phi) = |\vec{H}_{ext}|(\sin(\theta)\cos(\phi), \sin(\theta)\sin(\phi), \cos(\theta)).$$

The possible values for $\vec{H}_{ext}$ lie on the surface of a sphere, which we call control space $\mathcal{C}$.
In the following we set $q = 1$ and $|\vec{H}_{ext}| = 1$.

Using Brownian dynamics, we simulate the movement of a point dipole with the following equation of motion

$$\xi\dot{x}_{\mathcal{A}}(t) = -\nabla_{\mathcal{A}} V(x_{\mathcal{A}}, \vec{H}_{ext}(t)) + \eta(t),$$

where t is the time, $x_{\mathcal{A}}$ is the position of the dipole in $\mathcal{A}$, ξ is the friction coefficient and η is a Gaussian random force with a variance given by the fluctuation-dissipation theorem.
V is the potential, given by

$$V = \vec{H}_{ext}(t) \cdot \vec{H}_{pat}(\vec{x}_{\mathcal{A}}),$$

where

$$\vec{H}_{pat}(x_{\mathcal{A}}) = \sum_{j=1}^{5} \begin{pmatrix} \vec{q}_{2_j} \sin(\vec{q}_{2_j} \cdot \vec{x}_{\mathcal{A}}) \\ |\vec{q}_{2_j}| \cos(\vec{q}_{2_j} \cdot \vec{x}_{\mathcal{A}}) \end{pmatrix}.$$

The gradient of V is calculated with the symmetric difference quotient:

$$(\nabla_{\mathcal{A}} V(\vec{x}_{\mathcal{A}}))_i = \frac{V(\vec{x}_{\mathcal{A}} + \vec{h}_i) - V(\vec{x}_{\mathcal{A}} - \vec{h}_i)}{2h},$$

where $h = 1 \cdot 10^{-6}$ and $\vec{h}_i = h(\delta_{i1}, \delta_{i2})$, $i = 1, 2$.
The later needed derivatives of $\vec{H}_{pat}$ are calculated equivalently.

We integrate the equation of motion with the Euler algorithm:

$$\vec{x}_{\mathcal{A}}(t + \Delta t) = \vec{x}_{\mathcal{A}}(t) - \nabla V \Delta t/\xi + \delta\vec{r},$$

where Δt is the time step and $\delta\vec{r}$ is a random displacement sampled from a gaussian distribution with standard derivation $\sqrt{(2\Delta t k_B T/\xi)}$. Here k_B is the Boltzmann constant and T the absolute temperature.
As fundamental units we choose the diameter of the colloids $\sigma = 1$, the energy $\epsilon = 1$ and the friction $\xi = 1$. Thus the derived units are the time $\tau = \frac{\sigma^2\xi}{\epsilon}$ and the force $f = \frac{\epsilon}{\sigma}$.
The effective temperature is $T^* = \frac{k_B T}{\epsilon}$. For the simulations we set $T^* = 1 \cdot 10^{-7}$, because we are interested in adiabatic motion and thus we need the random displacement to be small.
In all simulations the time step is $\Delta t = 5 \cdot 10^{-5}$.
To generate the random displacement, we use the Box-Muller transformation.

As a test for the simulation code, we have calculated the known results for a lattice with 6-fold symmetry. Doing this, we have completely reproduced the phase diagramm in [3], figure 2.

4 Controlling one particle

In order to transport a single colloid along a given path on the quasicrystal, we discretise the path and calculate for every point of the path the external field which makes the point stationary.

We can desrcibe the system analogue to the system with a 6-fold lattice, compare [3], since the systems are equivalent upto the potential.
$\vec{x}_{\mathcal{A}}$ is a stationary point of $\vec{H}_{ext}$ if $\nabla V(\vec{x}_{\mathcal{A}}) = 0$. We write $\vec{H}^{(s)}_{ext}(\vec{x}_{\mathcal{A}})$ for the field which makes $\vec{x}_{\mathcal{A}}$ a stationary point. $\vec{H}^{(s)}_{ext}$ can be calculated as follows:

$$\vec{H}^{(s)}_{ext}(\vec{x}_{\mathcal{A}}) = \partial_1 \vec{H}_{pat}(\vec{x}_{\mathcal{A}}) \times \partial_2 \vec{H}_{pat}(\vec{x}_{\mathcal{A}}).$$

With this, the Hessian matrix of the potential is:

$$\nabla\nabla V = \begin{pmatrix} \vec{H}^{(s)}_{ext} \cdot \partial_1\partial_1 \vec{H}_{pat} & \vec{H}^{(s)}_{ext} \cdot \partial_1\partial_2 \vec{H}_{pat} \\ \vec{H}^{(s)}_{ext} \cdot \partial_2\partial_1 \vec{H}_{pat} & \vec{H}^{(s)}_{ext} \cdot \partial_2\partial_2 \vec{H}_{pat} \end{pmatrix}$$

If $\det \nabla\nabla V(\vec{x}_{\mathcal{A}}) > 0$, there are two saddle points and if $\det \nabla\nabla V(\vec{x}_{\mathcal{A}}) < 0$, there is a maximum and a minimum of the potential. Since we are interested in adiabatic motion, our colloid should always be in a minimum of the potential, i.e. it should only be transported along points which satisfy $\det \nabla\nabla V(\vec{x}_{\mathcal{A}}) < 0$. We call a set of points which fulfill $\det \nabla\nabla V(\vec{x}_{\mathcal{A}}) < 0$ an allowed region and a set of points which fulfill $\det \nabla\nabla V(\vec{x}_{\mathcal{A}}) > 0$ a forbidden region.
If $\det \nabla\nabla V(\vec{x}_{\mathcal{A}}) = 0$, the two saddle points become a maximum and a minimum of the potential or vice versa. We call a set of points which satisfy $\det \nabla\nabla V(\vec{x}_{\mathcal{A}}) = 0$ a **fence**.
An allowed area which is completely enclosed by fences is called a **home**.

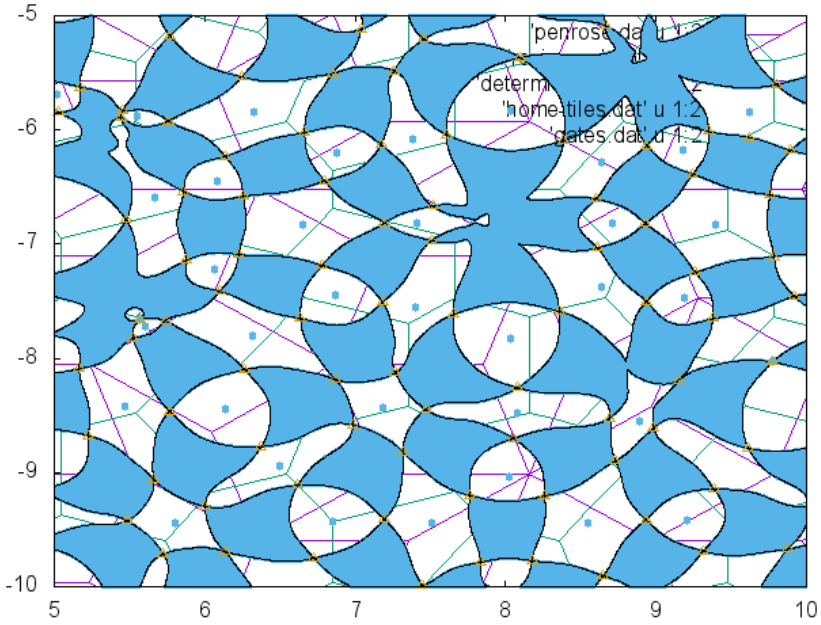

Figure 3: A patch of the quasicrystal with forbidden regions (blue), fences (black), gates (orange) and homes (white areas). In the background one can see the Delone tiling in purple and the Voronoi tiling in green. The axes tiling is in units of $2\pi/q$.

In figure 3 the allowed regions are the white areas and the fences are the black lines. The point of contact between two homes is called **gate**. The gates are the orange triangles and the centres of the homes (or the centre of its adjacent gates, to be more exact) are marked with blue squares.
It is remarkable that figure 3 implicates no obvious connection between the alloowed areas and the quasicrystal or the Penrose tiling, respectively. Thus the discussion in this section and in section 5.1 depends only on the potential. But surely the potential is connected with the used quasicrystal via the star vectors, which appear, upto a scaling factor, in $\vec{H}_{pat}$ and thus in the potential. However, the used shift vector does not appear in the potential.

In the following we transport a colloid by two homes. As path we use the linear connections between adjacent gates and homes, as shown in figure 4. Let the uppest marked home in figure 4, the 'fish', be home 1, the one in the middle home 2, and the home where the path ends home 3.
We enumerate the gate between two homes a and b as gate $a|b$. Thus our path consists of the linear connections (home 1 - gate 1|2), (gate 1|2 - home 2), (home 2 - gate 2|3) and (gate 2|3 - home 3), where we identify each home with its centre.
Such a path is completely contained inside the allowed areas, if all linear connections between the gates and homes along the path are inside the allowed areas. This is the case for nearly all homes, especially for the homes 1, 2 and 3. But for a general path one should keep in mind to check this condition, or study what happens if the path crosses the forbidden area.

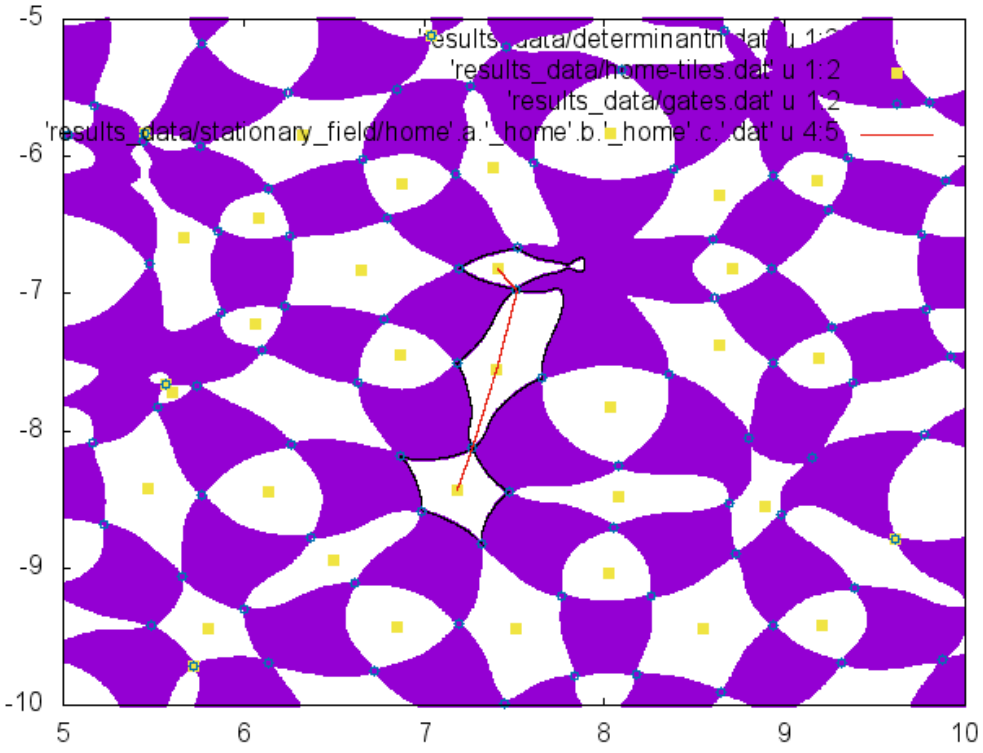

Figure 4: The red line marks the given path from home 1 via home 2 to home 3. The path follows the linear connections between a home and an adjacent gate along the allowed area. The axes tiling is in units of $2\pi/q$.

As earlier stated, the maximum and the minimum of the potential become two saddle points if we cross a fence. This causes problems when we calculate $H_{ext}^{(s)}$ while out path crosses a gate, because at every gate meet two fences. This leads to the problem that maximum and minimum of the potential change at a gate. Since the external fields which lead to the maximum and the minimum of the potential, respectively, are on the opposite side of $\mathcal{C}$, we have to invert the calculated external field in every second home.
(...)

At this point a consistence check is useful, since the external field which stabilizes a given point $x_{\mathcal{A}} \in \mathcal{A}$ is not unique; if H_{ext}^{s} stabilizes $x_{\mathcal{A}}$, the same holds for $-H_{ext}^{s}$. We show two such tests in figure 5.

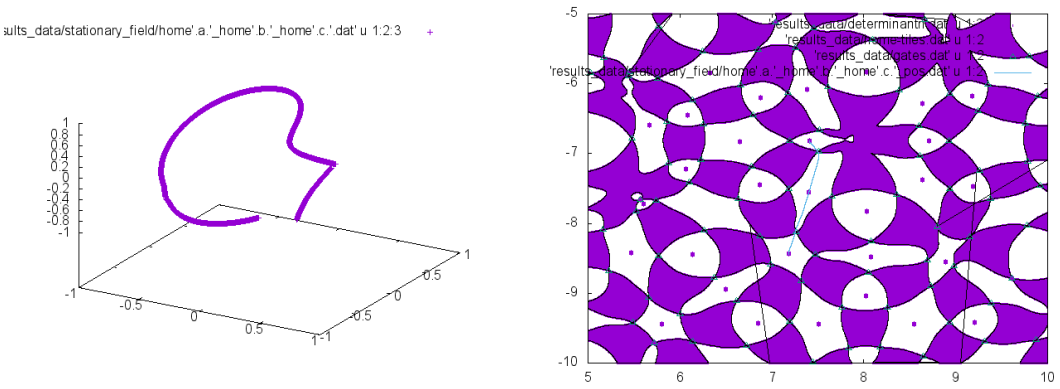

Figure 5: Left: As it should be, the calculated external field varies on the surface of the unit sphere. Right: If we use the calculated external field and calculated the path it leads to, we obtain the path we started with, cf. figure 4.
Note that the fences which look wrong in the figure are due to some problems with the calculated data and have no physical meaning.

5 Controlling two or more particles

5.1 Idea 1: Constructing paths on $\mathcal{C}$

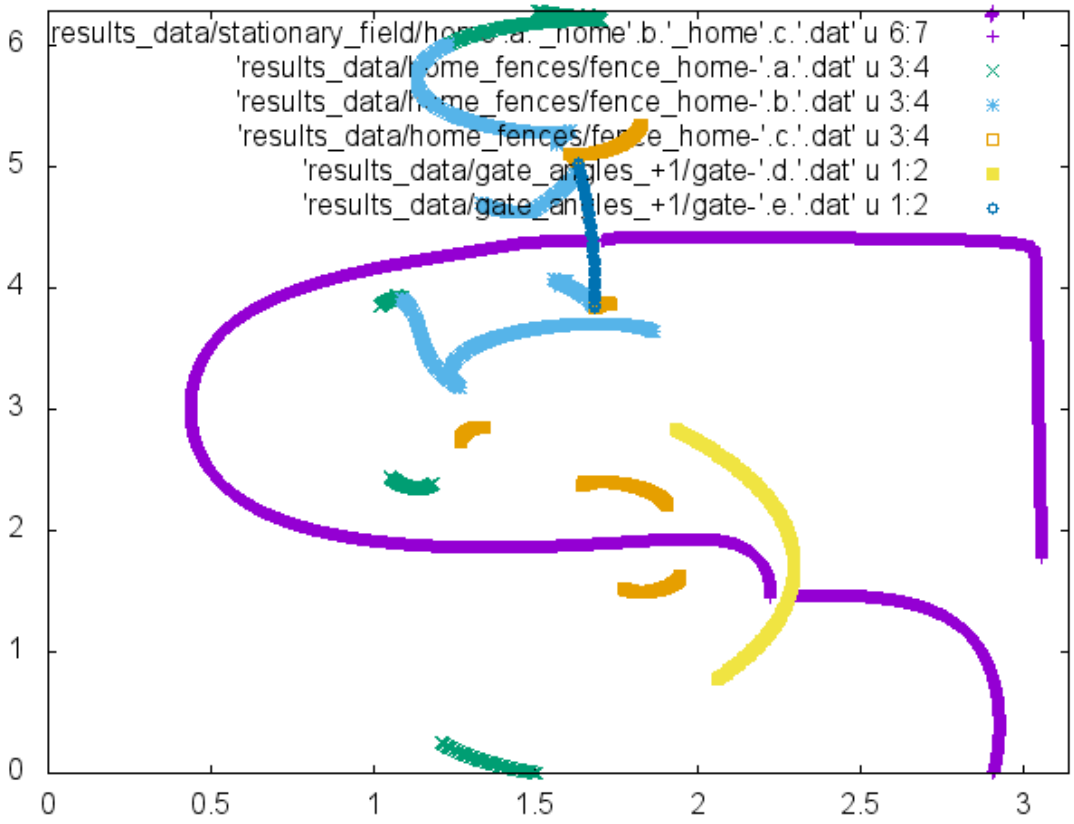

Figure 6: The purple line marks the calculated external field. The yellow and dark blue lines are the projections of the gates 16/17 and 17/20 onto $\mathcal{C}$, and the green, the blue and the orange lines are the projections of the fences around the homes 16, 17 and 20 onto $\mathcal{C}$. On the x-axis varies θ and on the y-axis ϕ.

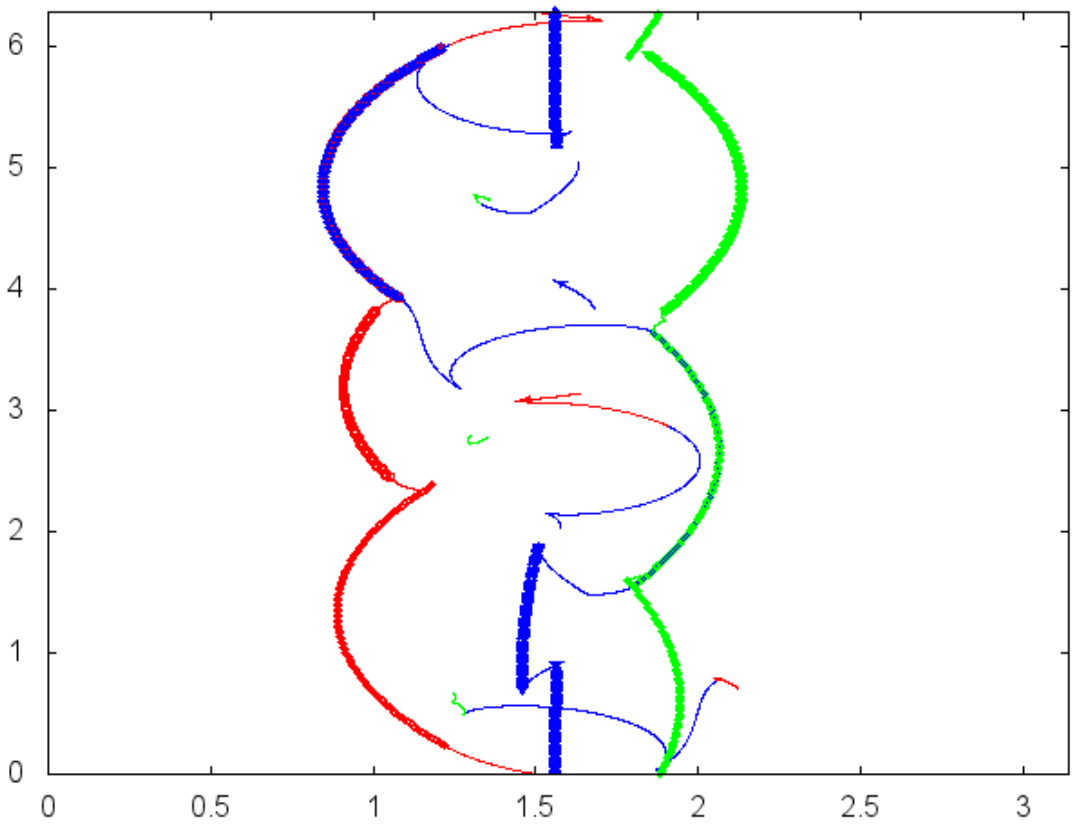

Figure 7: The thick lines are the projections of all gates adjacent to a home onto $\mathcal{C}$ and the thin lines are the projections of the fences around a home. For technical reasons, each fence appears twice. The correct fences are those who are connected with a gate of the same color. Red marks home 17, blue marks home 16 and green marks home 15. On the x-axis varies θ and on the y-axis ϕ.

5.2 Idea 2: Inner space $\mathcal{E}^{\perp}$

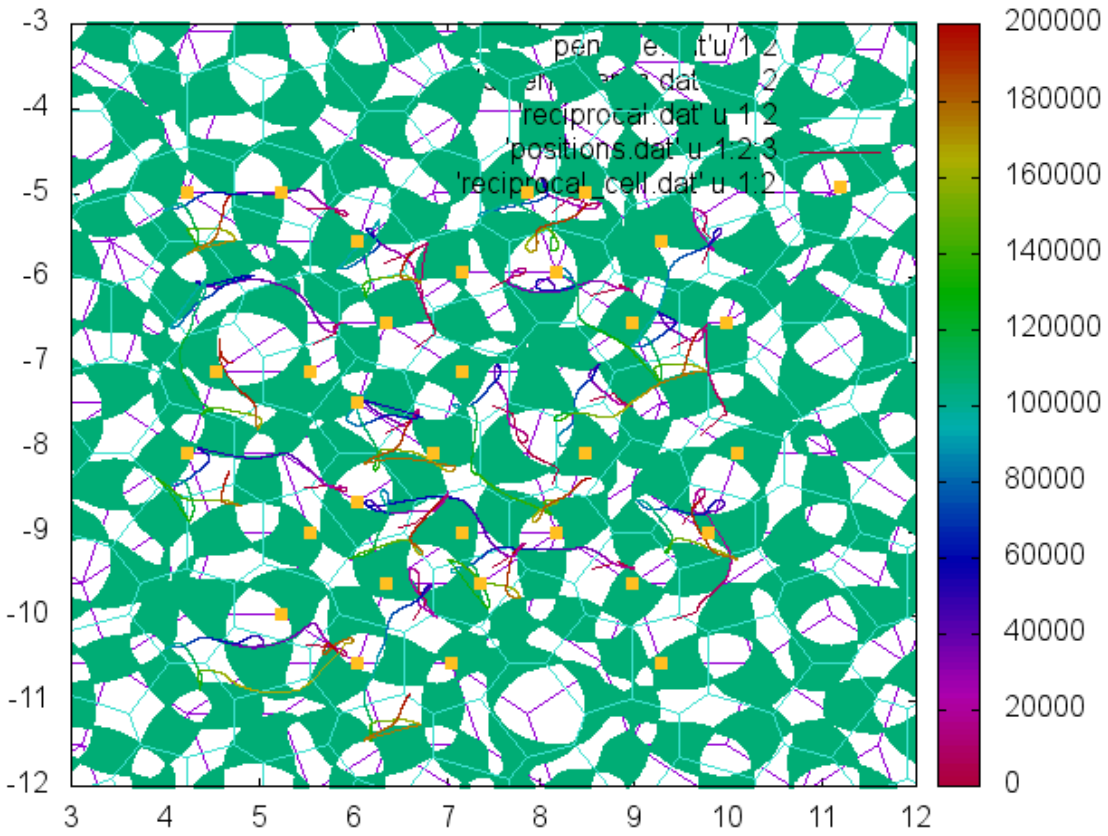

Figure 8: The thick lines are the projections of all gates adjacent to a home onto $\mathcal{C}$ and the thin lines are the projections of the fences around a home. For technical reasons, each fence appears twice. The correct fences are those who are connected with a gate of the same color. Red marks home 17, blue marks home 16 and green marks home 15. On the x-axis varies θ and on the y-axis ϕ.

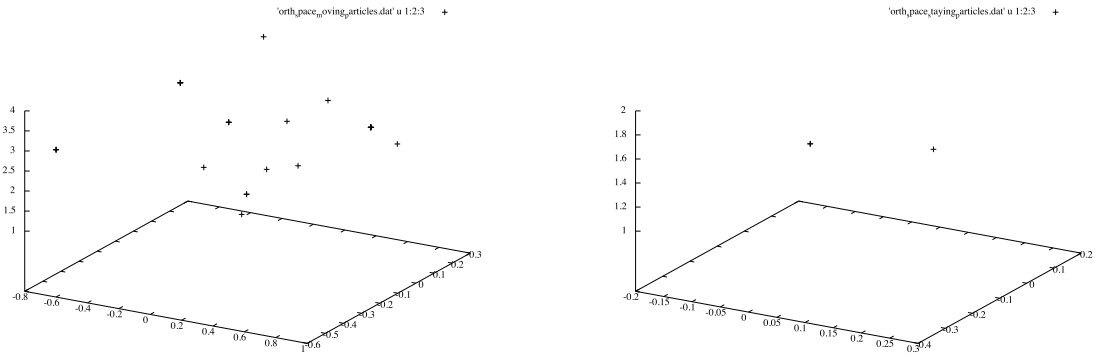

Figure 9: Left: Projections onto $\mathcal{E}^{\perp}$ of the (Voronoi-)cells in which the trajectory of a colloid ended, if it started in another one.
Right: Projections onto $\mathcal{E}^{\perp}$ of the (Voronoi-)cells in which a trajectory started and ended, i.e. of the cells with staying colloids.

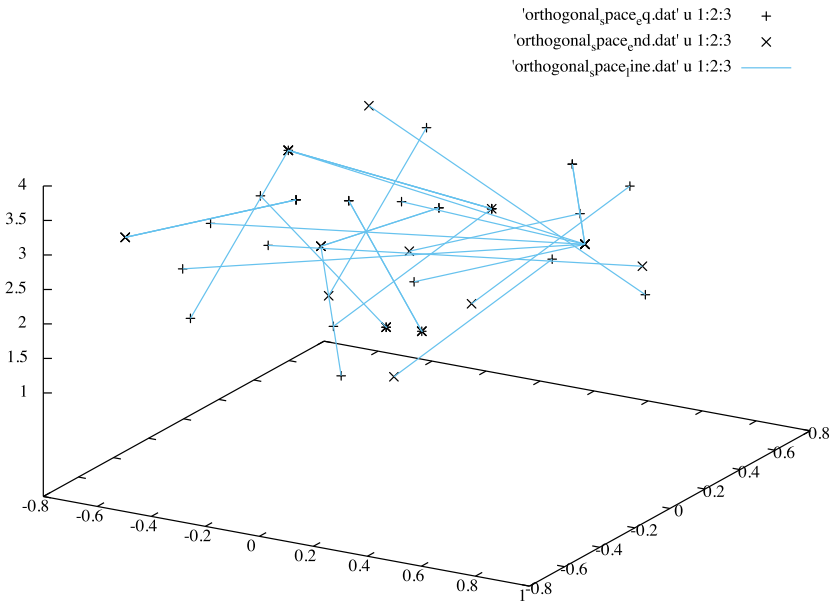

Figure 10: The '+' mark the starting positions and the 'x' the endpositions. Thus a 'star' marks a cell in which a colloid started and (eventually a different one) ended. The blue lines connect corresponding pairs of starting- and endpositions.

6 Conclusions

War gut.

I want to thank my supervisors Dr. Daniel de las Heras, Prof. Matthias Schmitt, Prof. Michael Lönne and Prof. Thomas Fischer that they enabled me to do both bachelor thesis in one interdisciplinary project in maths and physics.
It was the try of something new and thus surely made some more work for the supervisors than two seperate bachelor thesis would have. Thus a special thanks goes to Dr. Daniel de las Heras and Prof. Thomas Fischer who had the idea for the project and ensured that it would be working formally (in law) and in content.

It is sad that there was no possibility to submit the interdisciplinary project as one interdisciplinary thesis in maths and physics, due to problems with the law. Today universities and politics want the scientists to work interdisciplinary, but it is not possible to submit an interdisciplinary project as such?!

Nevertheless this was exactly what i was looking for: a project in which i could study a topic mathematically and physically.

References

[1] D. de las Heras et al. Topologically protected colloidal transport above a square magnetic lattice. *New Journal of Physics*, 2016.

[2] T. Lebeda. Mathematical properties of quasicrystals and the influence of the projection window, 2016.

[3] J. Loehr et al. Topological protection of multiparticle dissipative transport. *Nat. Comm.*, 2016.

[4] M. Senechal. *Quasicrystals and geometry*. Cambridge University Press, 1995.

Erklärung

Hiermit bestätige ich, dass ich die vorliegende Arbeit selbst verfasst, nur die angegebene Literatur als Hilfsmittel verwendet habe und alle wörtlich oder sinngemäß übernommenen Äußerungen anderer Autoren gekennzeichnet habe. Außerdem versichere ich, dass ich die Arbeit zu keinem früheren Zeitpunkt bereits zur Erlangung eines akademischen Grades eingereicht habe.

Bayreuth, den 26.11.2016

_____

TIMO LEBEDA